Transactions, SMiRT-22
San Francisco, California, USA - August 18-23, 2013
Division IV

GENERATION OF PUMP-INDUCED PULSATION LOADS FOR THE AP1000 REACTOR INTERNALS

Gregory A. Banyay[1], Gregory M. Imbrogno[2], Gregory A. Meyer[3]

[1] Senior Engineer, Westinghouse Electric Company, Cranberry Township, PA (banyayga@westinghouse.com)
[2] Principal Engineer, Westinghouse Electric Company, Cranberry Township, PA
[3] Principal Engineer, Westinghouse Electric Company, Cranberry Township, PA

ABSTRACT

Four motor-driven centrifugal reactor coolant pumps provide coolant flow for the Westinghouse **AP1000®** reactor. The pumps provide a periodic fluid-borne acoustic excitation to the closed-loop reactor coolant system at frequencies corresponding to the shaft and blade passing rates. That acoustic excitation is one source of flow-induced vibration that structural and fatigue evaluations of components within the reactor coolant system, including the reactor vessel internals, must consider. A node and flow path formulation based acoustic code known as ACSTIC2 is used to model the fluid mechanics. Multiple technical challenges must be traversed in order to accurately calculate pump-induced pulsation loads. Those challenges include quantifying and modeling the pump source term amplitude, modeling hydrodynamic damping, quantifying uncertainty, and coupling acoustic loads with the structure. First, a method of empirically determining the pump source term amplitude and subsequent scaling of that amplitude for off-normal operating conditions is discussed. Second, various methods of modeling hydrodynamic damping of the acoustic phenomena is discussed and a suggestion for improvement is made for Section III Appendix N of the ASME Boiler and Pressure Vessel Code. Third, the applicability of traditional uncertainty analysis techniques is presented for an acoustic analysis. Finally, a method of coupling the acoustic loads to the structure is presented and potential opportunities for more strongly coupling the acoustic and structural domains are discussed.

NOMENCLATURE

c	Sound Speed
p	Pressure Amplitude
ϕ	Phase Angle
Δp	Pressure Difference
Δp_B	Body Force Pressure Difference
w	Mass Flowrate
ω	Rotational Velocity
E_v	Bulk Modulus
ρ	Density
v	Velocity
V	Volume
L/A	Length to Area Ratio, Inertial Term
K/A^2	Hydraulic Loss Factor to Area Squared Ratio, Viscous Term
m	Flow Path Number
n	Node Number
H	Head Pressure

h	Pump Pulsation Head Amplitude
Q	Volumetric Flowrate
ζ	Damping Ratio
η	Coefficient of Shear Viscosity
η_B	Coefficient of Bulk Viscosity
t	Time
T	Temperature
γ	Wave Number
S	Simulation Result (Uncertainty)
X_i	Significant Input Parameter (Uncertainty)
u_{xi}	Corresponding Standard Uncertainty in Input Parameter X_i (Uncertainty)
z	Position Vector (Uncertainty)
θ_i	Sensitivity coefficient for the ith significant input (Uncertainty)

INTRODUCTION

Flow-Induced Vibration (FIV) loading can significantly contribute to structural and fatigue evaluations of components within a Reactor Coolant System (RCS). Sources of FIV include turbulence, vortex shedding, fluid-elastic instability, and acoustics. A significant contributor to FIV acoustic loading in a Pressurized Water Reactor (PWR) RCS, such as the Westinghouse AP1000 plant, is the Reactor Coolant Pump (RCP). The Westinghouse AP1000 plant is a two-loop design in which there are four cold legs and two hot legs. Each hot leg supplies a steam generator to which two RCP's are mounted that supply coolant flow to the cold legs and thus the reactor. Each motor-driven RCP incorporates a seven-blade centrifugal impeller. The RCP has an acoustic pulsation signature, particularly at the rates associated with the shaft and blade-passing frequencies, and twice thereof, which is used as a forcing function for FIV analysis. That pulsation signature is usually determined empirically though recently analytical investigations have been made to this end.

That forcing function is modeled as a body force amplitude pressure difference within the context of the node and flow-path formulation of the ACSTIC2 program. The ACSTIC2 program is used to discretize the RCS such that the acoustic wave could be resolved. The ACSTIC2 analysis results in pressure amplitudes in regions of interest or pressure differences across components of interest and the associated phase angle, as a function of frequency. The governing equations are described in [1] and may be summarizes as follows:

Given the un-damped wave equation:

$$\nabla^2 p = \frac{1}{c^2}\frac{\partial^2 p}{\partial t^2} \quad (1)$$

The fluid momentum and mass conservation equations may be used to model the acoustic pulsation as follows:

$$\left[i\omega \sum_{i=1}^{n} \frac{L_i}{A_i} + \frac{w}{\rho}\sum_{i=1}^{n} \frac{K_i}{A_i^2}\right] w - \Delta p = \Delta p_B \quad (2)$$

$$i\omega p - \frac{c^2}{V}\sum_{j=1}^{m} w_j = 0 \quad (3)$$

PUMP FORCING FUNCTION CHARACTERIZATION

A scale model RCP was tested at full speed and constant temperature in a piping loop and the pulsation characteristic was measured at the four rates of interest (1 and 2 times the shaft frequency, and 1 and 2 times the blade-passing frequency). Given that the test was conducted on a scale model RCP at full speed and constant temperature, it was necessary to scale the test results for analytical modeling of the full-scale RCP operating at various speeds and temperatures.

Pump head-flow performance curves may be non-dimensionalized per [12] as follows:

$$Head\ vs.\ Flow \rightarrow \left(\frac{H}{H_r}\right)\cdot\left(\frac{\omega_r}{\omega}\right)^2\ vs.\left(\frac{Q}{Q_r}\right)\cdot\left(\frac{\omega_r}{\omega}\right) \qquad (4)$$

Where the subscript "r" indicates a reference value, $\left(\frac{H}{H_r}\right)\cdot\left(\frac{\omega_r}{\omega}\right)^2$ may be considered dimensionless head, and $\left(\frac{Q}{Q_r}\right)\cdot\left(\frac{\omega_r}{\omega}\right)$ may be considered dimensionless flow. Pumps generally follow a relationship like:

$$\left(\frac{H}{H_r}\right)\cdot\left(\frac{\omega_r}{\omega}\right)^2 = F\left(\left(\frac{Q}{Q_r}\right)\cdot\left(\frac{\omega_r}{\omega}\right)\right) \qquad (5)$$

Where *F* is an experimentally determined function. The dimensionless head parameter is related to the angle of attack of the impeller blade through the fluid. For pump pulsation head amplitudes, h, a similar relationship holds because the fluctuations are caused by the passage of the impeller blade through the fluid and should therefore be proportional to impeller rotational speed squared. To extrapolate from scale model test to a full size representation, the following relationship is used:

$$h/_{(R\cdot\omega)^2} = G\left(V/_{(R\cdot\omega)}\right) \qquad (6)$$

Where *G* is another experimentally determined function and R is a scale factor based on the relative size of the scale model. If *R* is interpreted as a normalized impeller radius, the ratio $V/_{(R\cdot\omega)}$ is simply a ratio of rotational and linear velocities and is related to the angle of attack, as before. The angle of attack will therefore be equivalent for the scale model and full scale if the $V/_{(R\cdot\omega)}$ is the same for the scale model and full scale.

The $R\omega$ factor appears on the left-hand side of (6) and so head is proportional to the square of the velocity as is the case in (5). Therefore, to use scale model data to generalize to full scale, the following ratio may apply based on a given full scale operating point:

$$\frac{\left[h/_{(R\cdot\omega)^2}\right]_{full}}{\left[h/_{(R\cdot\omega)^2}\right]_{scale}} = \frac{\left[G\left(V/_{(R\cdot\omega)}\right)\right]_{full}}{\left[G\left(V/_{(R\cdot\omega)}\right)\right]_{scale}} \qquad (7)$$

If a scale model data point for which is the same for full scale and the scale model, then the right-hand side of (7) becomes unity and:

$$\left[h/_{(R\cdot\omega)^2}\right]_{full} = \left[h/_{(R\cdot\omega)^2}\right]_{scale} \qquad (8)$$

Finally, in order to apply Equation (8) in terms of pressure units rather than head, the scale model test density and the desired full scale density shall be considered. So, the density correction implicitly handles the impact of temperature variation between scale model pulsation and desired full scale pulsation.

$$\left[\Delta p_B \Big/ (\rho \times (R \cdot \omega)^2)\right]_{full} = \left[\Delta p_B \Big/ (\rho \times (R \cdot \omega)^2)\right]_{scale} \quad (9)$$

Thus, Equation (9) is used as the basis for converting representative full scale pulsation forcing functions from scale model test results. Two factors not considered by this approach are non-linear temperature sensitivity as described in [8] and variations in pulsation at pump speeds away from the pumps' best-efficient point as described in [7].

ACOUSTIC HYDRODYNAMIC DAMPING

Subsection N-1470 of [14] addresses hydrodynamic damping with respect to a coupled fluid-shell system. While that discussion is necessary and warranted, damping formulations within the fluid medium itself lack consensus. The following discussion illustrates some level of the variety of methods that can be used to model acoustic fluid damping and attempts to establish come commonality among methods.

Acoustic damping is discussed in [13] and the loss mechanisms may be categorized as viscous losses, heat losses, or losses due to molecular exchanges of energy. Per [13], the viscous losses result from relative motion occurring between various portions of the medium during the compressions and expansions that accompany the transmission of a sound wave.

One formulation of the damped wave equation is presented in the 4th edition of [13] as:

$$\left(1 + \tau_s \frac{\partial}{\partial t}\right) \nabla^2 p = \frac{1}{c^2} \frac{\partial^2 p}{\partial t^2} \quad (10)$$

Where:

$$\tau_s = \left(\frac{4}{3}\eta + \eta_B\right) \Big/ \rho c^2$$

Another formulation is presented in the ANSYS user's manual [16] as:

$$\nabla \cdot \left(\frac{1}{\rho} \nabla p\right) + \nabla \cdot \left[\frac{4\mu}{3\rho} \nabla \left(\frac{1}{\rho c^2} \frac{\partial p}{\partial t}\right)\right] = \frac{1}{\rho c^2} \frac{\partial^2 p}{\partial t^2} \quad (11)$$

In the 1st edition of [13], the dissipative forces are incorporated in the fluid equation of motion (momentum) with an R'u term as (in 1-D):

$$-\frac{\partial \mathrm{p}}{\partial \mathrm{x}} = \rho \frac{\partial v}{\partial t} + R'u \quad (12)$$

Equation (12) is similar to the momentum equation upon which ACSTIC2 is programmed except that R' is replaced by $\rho \times RESP$, where the RESP parameter to handle viscous damping effects is defined as:

$$RESP = \frac{w}{\rho \times \left(\sum_{i=1}^{N} \frac{L_i}{A_i}\right)} \left(\sum_{i=1}^{N} \frac{K_i}{A_i^2}\right) \quad (13)$$

Assuming that independent variables are harmonic (i.e., vary as $e^{i\omega t+\gamma x}$), the following characteristic equation is obtained:

$$\omega^2 - i\omega \cdot RESP - c^2\gamma^2 = 0 \quad (14)$$

Where:

$$\gamma = \pm\left(\frac{\omega}{c}\right)\sqrt{1 - i\frac{R'}{\rho\cdot\omega}} = \pm\left(\frac{\omega}{c}\right)\sqrt{1 - i\frac{RESP}{\omega}} \approx \pm\left(\frac{\omega}{c}\right)\cdot\left(1 - i\frac{RESP}{2\omega}\right) \quad (15)$$

Solution of Equation (14) yields:

$$\omega = \left(i \cdot RESP \pm \sqrt{-RESP^2 + 4c^2\gamma^2}\right)\Big/_2$$

Critical damping ($\zeta = 1.0$) occurs when the expression under the radical is equal to zero.

$$RESP_0 = 2\omega = 4\pi f$$

Therefore, RESP may be expressed in terms of the damping ratio as:

$$RESP = 2\omega\zeta = 4\pi\zeta f \quad (16)$$

The damped acoustic wave equation may be expressed using RESP as:

$$\frac{1}{c^2}\frac{\partial^2 p}{\partial t^2} = -\nabla^2 p - \frac{RESP}{c^2}\frac{\partial p}{\partial t} \quad (17)$$

By re-arranging Equation (16) and substituting into Equation (15), the wave number may be expressed as:

$$\gamma \approx \pm\left(\frac{\omega}{c}\right)\cdot(1 - i\zeta) \quad (18)$$

Similarly, sound speed may be expressed in real and imaginary terms by using a δ term to modify the imaginary contribution to sound speed, where c_0 is the physical sound speed:

$$c = c_0(1 + i\delta) \quad (19)$$

Given that for a lightly damped system, $\omega \approx c\cdot\gamma$, Equations (18) and (19) are similar such that $\delta = \zeta$. Such a formulation allows an analyst to directly apply a known damping ratio which may be based on empirical data into an acoustic model under analysis.

Five damping options are available within ACSTIC2 as detailed in Table 1. Viscous damping incorporates the RESP term which is based on a known hydraulic loss and so is accurate for localized damping effects. The other types of damping are termed as such due to their analogy to structural dynamics. Mass damping is based on the general relationship for fluid systems that damping ratio varies inversely with frequency and so is accurate from a fluid system standpoint. Stiffness damping is the opposite from mass damping in the sense that damping ratio varies with frequency. Rayleigh damping combines the effects of mass and stiffness damping by use of the α and β terms. Finally, Hysteretic damping imparts a constant damping ratio independent of frequency which is of use in volumes through which significant flow does not pass such as a pressurizer.

Table 1 - Damping Formulations in ACSTIC2

Damping Type	Momentum[1] Particular form of (2)	Mass Conservation Particular form of (3)
Viscous	$w \cdot \sum_{i=1}^{N} \frac{L_i}{A_i}[i\omega + I_{RESP} \times RESP] - \Delta p = \Delta p_B$	$i\omega p - \frac{c^2}{V}\left(\frac{1}{i\omega}\right)\sum_{j=1}^{M} w_j = 0$
Rayleigh	Given $\left[\alpha = \frac{4\pi f_1 f_2(\zeta_1 f_2 - \zeta_2 f_1)}{f_2^2 - f_1^2}\right]$ and $\left[\beta = \frac{\zeta_2 f_2 - \zeta_1 f_1}{\pi(f_2^2 - f_1^2)}\right]$:	
	$w \cdot \sum_{i=1}^{N} \frac{L_i}{A_i}[i\omega + I_{RESP} \times RESP + \alpha] - \Delta p = \Delta p_B$	$i\omega p - \frac{c^2}{V}\left(\frac{1}{i\omega} + \beta\right)\sum_{j=1}^{M} w_j = 0$
Mass $\left(\zeta \propto \frac{1}{f}\right)$	$w \cdot \sum_{i=1}^{N} \frac{L_i}{A_i}[i\omega + I_{RESP} \times RESP + 4\pi\zeta_1 f_1] - \Delta p = \Delta p_B$	$i\omega p - \frac{c^2}{V}\left(\frac{1}{i\omega}\right)\sum_{j=1}^{M} w_j = 0$
Stiffness $(\zeta \propto f)$	$w \cdot \sum_{i=1}^{N} \frac{L_i}{A_i}[i\omega + I_{RESP} \times RESP] - \Delta p = \Delta p_B$	$i\omega p - \frac{c^2}{V}\left(\frac{1}{i\omega} + \frac{\zeta_1}{\pi f_1}\right)\sum_{j=1}^{M} w_j = 0$
Hysteretic	$w \cdot \sum_{i=1}^{N} \frac{L_i}{A_i}[i\omega + I_{RESP} \times RESP] - \Delta p = \Delta p_B$	$i\omega p - \frac{c^2}{V}\left(\frac{1}{i\omega} + \frac{2\zeta_1}{\omega}\right)\sum_{j=1}^{M} w_j = 0$

Notes:

1. I_{RESP} is a switch that can be turned on in ACSTIC2. Usually, $I_{RESP} = 1$ for Viscous damping and $I_{RESP} = 0$ for all other types.

UNCERTAINTY QUANTIFICATION

Section 3 of ASME V&V 20 [15] presents a methodology for calculating the effect of input parameter uncertainty on simulation uncertainty. That document is intended to address computational fluid dynamics and heat transfer analyses. While the pump pulsation acoustic analysis described in this paper should not be considered equivalent to computational fluid dynamics, analogies may be drawn between the fields such that the general uncertainty methods are transferrable. The input uncertainty propagation equation is:

$$u_{input}{}^2 = \sum_{i=1}^{n_{inputs}} \left(\theta_i u_{x_i}\right)^2$$

Where:

$$\theta_i = \frac{\partial S(z,t,X)}{\partial X_i}$$

The central difference numerical differentiation scheme may be employed to establish the sensitivity coefficients if the amount by which the X_i input variable can vary is known:

$$\frac{\partial S}{\partial X_i} = \frac{S(X_1, X_2, \ldots, X_i + \Delta X_i, \ldots, X_n) - S(X_1, X_2, \ldots, X_i - \Delta X_i, \ldots, X_n)}{2\Delta X_i}$$

In the case of the ACSTIC2 analysis, the simulation result, S, is twofold in terms of both pressure and phase angle. Furthermore, the problem is solved in the frequency domain rather than the time domain. Therefore, the sensitivity coefficient for ACSTIC2 analysis may be defined as:

$$\theta_i = \begin{Bmatrix} \frac{\partial P(z,f,\boldsymbol{X})}{\partial X_i} \\ \frac{\partial \varphi(z,f,\boldsymbol{X})}{\partial X_i} \end{Bmatrix}$$

Four significant input parameters can be varied in the ACSTIC2 analysis to establish sensitivity. Therefore, the X vector becomes:

$$X = \begin{Bmatrix} c(E_v(T), \rho(T)) \\ \zeta(N) \\ \Delta p_B(f, N) \\ N \end{Bmatrix}$$

The sound speed term, *c*, is dependent on temperature, so the amount of expected temperature variation for a given analysis governs the fluid property variation. The damping ratio term, ζ, was based on the equations outlined above and experimental data such as that found in [2]. The body force amplitude, Δp_B, which is really the pump source term forcing function, is also based on experimental data as discussed above. The resultant pressure amplitudes and pressure differences vary in linear proportion to the magnitude of the source term forcing function. Finally, the RCP speed, *N*, is based on the range of possible operating speeds for the motor-driven pumps at a given plant operating condition. Furthermore, the RCP speed is input to ACSTIC2 by way of the frequency range of interest. ACSTIC2 sweeps through the frequency range of interest and produces results at each frequency (for the specified resolution).

INTERPRETATION OF ACOUSTIC LOADS AND FLUID-STRUCTURE INTERACTION

ACSTIC2 provides results in terms of pressure amplitude at a node or pressure difference between nodes. An example of a pressure difference between two nodes is shown in Figure 1. At the true frequency corresponding to the blade-passing rate (in this example), there is one resultant Δp. However, ACSTIC2 performs a sweep across a frequency range such that the result at a given location is really a function of frequency. Therefore, depending on the intended use of the analysis, the results may be interpreted differently. To ensure conservatism, the analyst may choose to use the maximum Δp within the Y% of nominal range. In a best-estimate analysis, the analyst may choose to use the maximum Δp within the X% of nominal range and employ uncertainty analysis techniques. Alternatively, the result could be interpreted in a spectral sense in which case the phase angle information is lost.

Another consideration is in coupling the acoustic load to the structure. The acoustic load could be taken on a component by component basis. For example, the maximum overall Δp at a given component could be found for all relevant ACSTIC node pairings. Then, the frequency associated with that overall Δp could be used as a basis for extracting all other acoustic Δp values for that component. Such a methodology would ensure continuity of the acoustic mode shape.

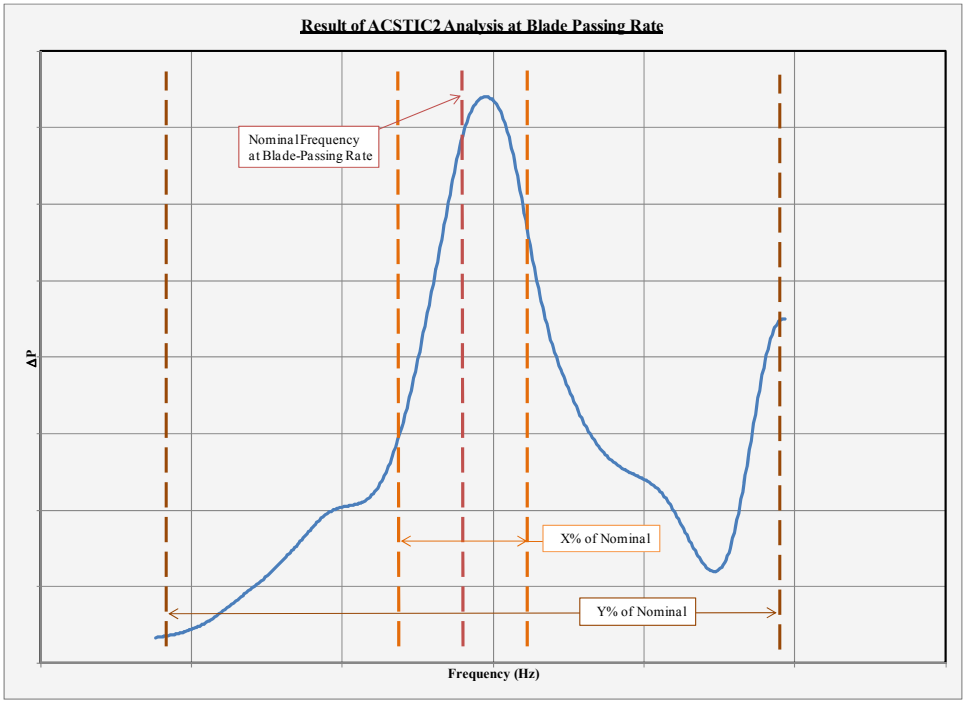

Figure 1 - Example ACSTIC2 Result for a Node Pairing

Modern numerical tools offer methods for strong coupling of the acoustic fluid and structural domains. For example, the ANSYS Fluid30 element offers a Lagrangian formulation of the acoustic wave equation using the Galerkin Finite Element Method. The following formulation is consistent with the work published by Everstine [17] and Zienkiewics [18]. The associated weak form is:

$$\int_{\Omega} \frac{1}{c^2}\delta P \cdot \frac{\partial^2 P}{\partial t^2}\, d\Omega + \int_{\Omega} (\nabla \delta P) \cdot (\nabla P)\, d\Omega = \int_{\Gamma} \vec{n}\delta P \cdot (\nabla P)\, d\Gamma$$

In order to couple the acoustic load to the structure, the boundary condition $\vec{n} \cdot \nabla P = -\rho_0 \vec{n} \cdot \frac{\partial^2 u}{\partial t^2}$ may be used to convert the fluid pressure to structural acceleration, in the direction normal to the structure. In such a case, the coupled weak form becomes:

$$\int_{\Omega} \frac{1}{c^2}\delta P \cdot \frac{\partial^2 P}{\partial t^2}\, d\Omega + \int_{\Omega} (\nabla \delta P) \cdot (\nabla P)\, d\Omega = -\int_{\Gamma} \rho_0 \delta P \vec{n} \cdot \left(\frac{\partial^2 u}{\partial t^2}\right) d\Gamma$$

Where the terms integrated in the Ω domain represent the continuum in the Γ domain are able to facilitate incorporation of the natural boundary conditions. By defining {N} as the matrix of shape functions and {B} as the associated spatial derivative, the following finite element equation may be formed:

$$\underbrace{\frac{1}{c^2}\int_{\Omega} \{N\}\{N\}^T\, d\Omega \{\ddot{P}_e\}}_{\text{Fluid Mass Matrix}} + \underbrace{\int_{\Omega} [B]^T[B]\, d\Omega \{P_e\}}_{\text{Fluid Stiffness Matrix}} + \underbrace{\rho_0 \int_{\Gamma} \{N\}\{n\}^T\{N'\}^T\, d\Gamma \{\ddot{u}_e\}}_{\text{Fluid/Structure Coupling Mass Matrix}} = \{0\}$$

In concise matrix form, the above equation becomes:

$$[M^P{}_e]\{\ddot{P}_e\} + [K^P{}_e]\{P_e\} + \rho_0[R_e]^T\{\ddot{u}_e\} = \{0\}$$

Correspondingly, in the structural domain, the equation of motion is:

$$[M_e]\{\ddot{u_e}\} + [C_e]\{\dot{u_e}\} + [K_e]\{u_e\} = \{F_e\} + \{F^{pr}{}_e\}$$

Where $\{F^{pr}{}_e\}$ represents the body force term associated with the fluid pressure. That term may be defined as:

$$\{F^{pr}{}_e\} = \int_\Gamma \{N'\}P\{n\}d\Gamma = \int_\Gamma \{N'\}\{N\}^T\{n\}d\Gamma\{P_e\} = [R_e]\{P_e\}$$

Where the $\int_\Gamma \{N'\}\{N\}^T\{n\}d\Gamma$ term matches the $[R_e]$ term in the fluid domain. By substitution and combining the structural and fluid equations, the following coupled equation may be formed, where the superscript "p" matrices are those formed by the acoustic fluid element:

$$\begin{bmatrix}[M_e] & [0]\\ \rho_0[R_e] & [M^p{}_e]\end{bmatrix}\begin{Bmatrix}\{\ddot{u_e}\}\\ \{\ddot{P}_e\}\end{Bmatrix} + \begin{bmatrix}[C_e] & [0]\\ [0] & [C^p{}_e]\end{bmatrix}\begin{Bmatrix}\{\dot{u_e}\}\\ \{\dot{P}_e\}\end{Bmatrix} + \begin{bmatrix}[K_e] & -[R_e]\\ [0] & [K^p{}_e]\end{bmatrix}\begin{Bmatrix}\{u_e\}\\ \{P_e\}\end{Bmatrix} = \begin{Bmatrix}\{F_e\}\\ \{0\}\end{Bmatrix}$$

By applying the finite element method to the acoustic fluid-structure interaction problem, commercial codes such as ANSYS can be used to solve the problem in an efficient manner.

Further advances to this finite element problem, including model order reduction [19] and an edge-based smoothed finite element method [20] have recently been proposed. Those advances offer improved computational efficiency and numerical stability to the problem at hand.

CONCLUSIONS

It has thus been shown that RCP acoustic pulsation loads were generated for the AP1000 plant's Reactor Internals by use of the ACSTIC2 program. The RCP source term was characterized based on scaling relationships from sub-scale test results, the fluid damping was explicitly modeled and tied to experimental data, the uncertainty and factors contributing thereunto were shown, and opportunities for incorporating fluid-structure interaction by way of finite elements was discussed.

REFERENCES

1. Schwirian, R.E.; Shockling, L.A.; Singleton, N.R.; Riddell, R.A. "Method for predicting pump-induced acoustic pressures in fluid-handling systems." Journal of Pressure Vessels and Piping (1982), 167-184.
2. Hartlen, R.T.; Urbanowicz, J.T.; Barreca, S.L. "Dynamic Interaction between Pump and Piping System." First International Pump Noise and Vibrations Symposium, Clamart, France, July 7-9, 1993.
3. Au-Yang, M.K., "Flow-Induced Vibration of Power and Process Plant Components: A Practical Workbook." Copyright © 2001 by the American Society of Mechanical Engineers.
4. Au-Yang, M.K., "Pump-Induced Acoustic Pressure Distribution in an Annular Cavity Bounded by Rigid Walls." Journal of Sound and Vibration (1979) **62**(4), 577-591, September 6, 1978.

5. Cheong, Jong-sik; Im, In-young; Oh, Seung-min; Baik, Se-jin. "An Analytical Prediction on the Pump-Induced Pressure Pulsation in a Pressurized Water Reactor." Transactions of the 15th International Conference on Structural Mechanics in Reactor Technology (SMiRT). 1999.
6. Min Kim, Kyung; In Le, Byoung; Lee, Donghwi; Hee Cho, Hyung, Seok Park, Jin; Hoon Jeong, Kyeong. "Pump-induced pulsating pressure distributions in a system-integrated modular reactor." Nuclear Engineering and Design (2012) 248, 216-225.
7. Corbo, Mark A.; Stearns, Charles, F. "Practical Design Against Pump Pulsations." Proceedings of the Twenty-Second International Pump Users Symposium. 2005.
8. Rzentkowski, G.; Zbroja, S. "Experimental Characterization of Centrifugal Pumps as an Acoustic Source at the Blade Passing Frequency." Journal of Fluids and Structures (2000) **14**, 529-558.
9. Penzes, L.E.; "Theory of Pump Induced Pulsating Coolant Pressure in Pressurized Water Reactor." Nuclear Engineering and Design (1974) **27**, 176-188.
10. Pavesi, G.; Cavazzini, G.; Ardizzon, G. "Time-Frequency Characterization of Rotating Instabilities in a Centrifugal Pump with a Vaned Diffuser." International Journal of Rotating Machinery (2008).
11. Langthjem, M.A.; Olhoff, N. "A numerical study of flow-induced noise in a two-dimensional centrifugal pump. Part II. Hydroacoustics." Journal of Fluids and Structures (2004) **19**, 369-386
12. I. J. Karassik, J. P. Messina, P. Cooper and C. C. Health. *Pump Handbook*, 4th ed. New York: McGraw-Hill, 2008.
13. Kinsler, L.E.; Frey, A.R. "Fundamentals of Acoustics." John Wiley & Sons, Inc.
14. ASME Boiler and Pressure Vessel Code, 2011 Edition, Section III, Appendix N.
15. ASME V&V 20-2009, Standard for Verification and Validation in Computational Fluid Dynamics and Heat Transfer.
16. Ansys 14.5 User Manual.
17. Everstine, G.C. "Finite Element Formulations of Structural Acoustics Problems," Computers and Structures, 1997.
18. Zienkiewics, O.C.; Taylor, R.L.; Zhu, J.Z. "Finite Element Method – Its Basis and Fundamentals," 6th Edition, Elsevier.
19. Puri, R.S.; Morrey, D.; Durodola, J.F. "A Comparison of Structural-Acoustic Coupled Reduced Order Models (ROMS): Modal Coupling and Implicit Moment Matching via Arnoldi," 14th International Congress on Sound & Vibration, 2007.
20. He, Z.C.; et al. "Coupled Analysis of 3D structural-acoustic problems using edge-based smoothed finite element method / finite element method," Finite Elements in Analysis and Design, 2010.
21. A.G. Piersol and T.L. Paez, "Harris Shock and Vibration Handbook," 6th Edition, McGraw-Hill, , 2010.
22. J.S. Bendat and A.G. Piersol, "Random Data: Analysis and Measurement Procedures," 4th Edition, John Wiley and Sons, 2010.
23. W. K. Bonness, J. B. Fahnline, and D. M. Jenkins, "Circumferential wavenumber decomposition of experimental data from structures containing circular symmetry," in *International Modal Analysis Conference 2003*, Paper # 184, 2003.

APPENDIX

The following is a suggested improvement to ASME Boiler & Pressure Vessel Code, Section III, Division 1, Appendix N-1400, "Dynamics of Coupled Fluid Shells:"

N-1440 ACOUSTIC FLUID MODES

N-1441 Analytical Methods

N-1441.1 Governing Equations

The un-damped acoustic wave equation in 3-D and 1-D, respectively are:

$$\frac{\partial^2 p}{\partial t^2} = c^2 \nabla p, \quad \text{in } \Omega$$

$$\frac{\partial^2 p}{\partial t^2} = c^2 \frac{\partial^2 p}{\partial x^2}, \qquad 0 \le x \le L$$

Carrying forward the 1-D formulation, for simplified conditions in which the acoustic pressure is zero at both ends of the domain:

$$p(0,t) = 0 \text{ and } p(L,t) = 0$$

and arbitrary initial conditions:

$$p(x,0) = f(x) \text{ and } \frac{\partial p}{\partial t}_{t=0} = g(x)$$

The series solution by separation of variables for the acoustic pressure is:

$$p_n(x,t) = (B_n \cos(\lambda_n t) + B_n{}^* \sin(\lambda_n t)) \sin\left(\frac{n\pi}{L}\right) x$$

where B is an arbitrary constant and λ is the eigenvalue, which is defined as:

$$\lambda_n = \frac{c(T) n\pi}{L}$$

where $c(T)$ is the temperature-dependent sound speed. A similar derivation could be done for other boundary conditions.

N-1441.2 Specific Case – Acoustic Modes of a Fluid Annulus bounded by Rigid Walls

{Insert the existing N-1440 and N-1441 here}

N-1442 Numerical Methods

The following finite element formulation is consistent with the work published by Everstine [17] and Zienkiewics [18]. The weak form for the acoustic wave equation is:

$$\int_\Omega \frac{1}{c^2} \delta P \cdot \frac{\partial^2 P}{\partial t^2} d\Omega + \int_\Omega (\nabla \delta P) \cdot (\nabla P)\, d\Omega = \int_\Gamma \vec{n} \delta P \cdot (\nabla P)\, d\Gamma$$

In order to couple the acoustic load to a structural acceleration, the boundary condition $\vec{n} \cdot \nabla P = -\rho_0 \vec{n} \cdot \frac{\partial^2 u}{\partial t^2}$ may be used to convert the fluid pressure to structural acceleration, in the direction normal to the face. In such a case, the coupled weak form becomes:

$$\int_\Omega \frac{1}{c^2} \delta P \cdot \frac{\partial^2 P}{\partial t^2} d\Omega + \int_\Omega (\nabla \delta P) \cdot (\nabla P)\, d\Omega = -\int_\Gamma \rho_0 \delta P \vec{n} \cdot \left(\frac{\partial^2 u}{\partial t^2}\right) d\Gamma$$

Where the terms integrated in the Ω domain represent the continuum in the Γ domain are able to facilitate incorporation of the natural boundary conditions. By defining $\{N\}$ as the matrix of shape functions and {B} as the associated spatial derivative, the following finite element equation may be formed:

$$\underbrace{\frac{1}{c^2}\int_\Omega \{N\}\{N\}^T d\Omega \{\ddot{P}\}}_{\text{Fluid Mass Matrix}} + \underbrace{\int_\Omega \{B\}^T\{B\} d\Omega \{P\}}_{\text{Fluid Stiffness Matrix}} + \underbrace{\rho_0 \int_\Gamma \{N\}\{n\}^T\{N'\}^T d\Gamma \{\ddot{u}\}}_{\text{Fluid/Structure Coupling Mass Matrix}} = \{0\}$$

In concise matrix form, the above equation becomes:

$$[M]\{\ddot{P}\} + [K]\{P\} + \rho_0 [R]^T \{\ddot{u}\} = \{0\}$$

In order to determine the fluid modes, let the above equation be homogeneous by making the forcing function equal to zero and setting *P* to be harmonic as follows.

$$\begin{matrix} [M]\{\ddot{P}\} + [K]\{P\} = \{0\} \\ \& \\ \{P\} = \{\varphi_i\}\cos(\omega_i t) \end{matrix} \quad \rightarrow \quad (-\omega_i{}^2[M] + [K])\{\varphi_i\} = \{0\} \quad \rightarrow \quad |[K] - \omega_i{}^2[M]| = 0$$

Therefore, the fluid modes may be determined by solving:

$$\omega = \pm\sqrt{[M]^{-1}[K]}$$

which may be solved easily by formulating the mass matrix in lumped form.

N-1442 Empirical Methods

In cases in which test data is available, the following methodology may be employed to determine acoustic modes.

Chapter 5 of [22] defines correlation, or covariance, functions as follows. A random process $x_k(t), -\infty < t < \infty$ is an ensemble of functions that can be characterized through its probability structure. For stationary random processes $x_k(t)$ and $y_k(t)$, the mean values become constants independent of *t*. So, for all *t*:

$\mu_x = E[x_k(t)] = \int_{-\infty}^{\infty} xp(x)dx$ and $\mu_y = E[y_k(t)] = \int_{-\infty}^{\infty} yp(y)dy$

where *p(x)* and *p(y)* are the probability density functions associated with the random variables $x_k(t)$ and $y_k(t)$, respectively.

The covariance functions of stationary random processes are also independent of t. For arbitrary fixed *t* and τ, the correlation functions are defined as:

$R_{xx}(\tau) = E[x_k(t)x_k(t+\tau)]$
$R_{yy}(\tau) = E[y_k(t)y_k(t+\tau)]$
$R_{xy}(\tau) = E[x_k(t)y_k(t+\tau)]$

where $R_{xx}(t)$ and $R_{yy}(t)$ are the autocorrelation functions of $x_k(t)$ and $y_k(t)$, respectively, whereas $R_{xy}(t)$ is the cross-correlation function between $x_k(t)$ and $y_k(t)$.

Chapter 19 of [21] describes the power spectral density (PSD) as follows. The fourier transform of a time sample of duration T (where $j = \sqrt{-1}$) is defined as:

$$X(f,t) = \int_0^T x(t)e^{-j2\pi ft}\,dt = \int_0^T x(t)\cos(2\pi ft)\,dt - j\int_0^T x(t)\sin(2\pi ft)\,dt$$

The PSD, also referred to as the autospectral density function, is the fourier transform of the autocorrelation function of a dynamic signal.

$$G_{xx}(f) = \lim_{T\to\infty}\frac{2}{T}E[|X(f,T)^2|], f > 0$$

where *E[]* denotes the expected value of *[]*, which implies an ensemble average. The PSD may then be plotted versus frequency to determine resonant modes.

Additionally, mode shapes identification may be facilitated by using techniques such as circumferential wavenumber decomposition, as described in [23].